11-25-1987

The refined crystal structure of a fully active semisynthetic ribonuclease at 1.8 Å resolution

Philip D. Martin
Department of Biochemistry, Wayne State University School of Medicine

Marilynn S. Doscher
Department of Biochemistry, Wayne State University School of Medicine

Brian FP Edwards
Department of Biochemistry, Wayne State University School of Medicine, bedwards@med.wayne.edu

Recommended Citation

Martin, P. D., Doscher, M. S., and Edwards, B. F. P. The refined crystal structure of a fully active semisynthetic ribonuclease at 1.8 Å resolution, J. Biol. Chemistry 262: 15930-15938, 1987. https://doi.org/10.1016/s0021-9258(18)47678-8

The Refined Crystal Structure of a Fully Active Semisynthetic Ribonuclease at 1.8-Å Resolution*

Philip D. Martin, Marilynn S. Doscher, and Brian F. P. Edwards

From the Department of Biochemistry, Wayne State University School of Medicine, Detroit, Michigan 48201

A fully active, semisynthetic analog of bovine ribonuclease A, comprised of residues 1–118 of the molecule in a noncovalent complex with the synthetic peptide analog of residues 111–124, has been crystallized in space group P3$_2$21 from a solution of 1.3 M ammonium sulfate and 3.0 M cesium chloride at pH 5.2. The crystallographic structure was determined by rotation and translation searches utilizing the coordinates for ribonuclease A reported by Wlodawer and Sjolin (Wlodawer, A., and Sjolin, L. (1983) *Biochemistry* 22, 2720–2728) and has been refined at 1.8-Å resolution to an agreement factor of 0.204. Most of the structure of the semisynthetic enzyme closely resembles that found in ribonuclease A with the synthetic peptide replacing the C-terminal elements of the naturally occurring enzyme. No redundant structure is seen; residues 114–118 of the larger chain and residues 111–113 of the peptide do not appear in our map. The positions of those residues at or near the active site are very similar to, if not identical with, those previously reported by others, except for histidine 119, which occupies predominantly the B position seen as a minor site by Borkakoti *et al.* (Borkakoti, N., Moss, D. S., and Palmer, R. A. (1982) *Acta Crystallogr. Sect. B Struct. Crystallogr. Cryst. Chem.* 38, 2210–2217) and not at all by Wlodawer and Sjolin (1983).

Successive digestion of bovine pancreatic RNase A[1] by pepsin and by carboxypeptidase A removes 6 residues from the C terminus of the molecule (residues 119–124), leaving RNase 1–118, a polypeptide that is without enzymatic activity (Lin, 1970). Complementation of RNase 1–118 with a synthetic tetradecapeptide comprising the C terminus of RNase, *viz.* residues 111–124, provides a semisynthetic, noncovalent complex, RNase 1–118·111–124, which exhibits 98% of the enzymatic activity of RNase A (Lin *et al.*, 1970; Gutte *et al.*, 1972). The titration behavior of the 4 histidine residues in the complex (including active site histidines 12 and 119) as revealed by proton NMR measurements is indistinguishable from that observed for these residues in RNase A (Doscher *et*

al., 1983a). Because any amino acid in the tetradecapeptide can be changed at will, RNase 1–118·111–124 is an excellent system for exploring the functions of these residues by the chemical equivalent of site-directed mutagenesis.

Several analogs of the complex have been synthesized to test postulated roles for Phe-120, Asp-121, and Ser-123 in the mechanism of action of the enzyme (Lin *et al.*, 1972; Hodges and Merrifield, 1974, 1975; Stern and Doscher, 1984). Roles for both Phe-120 and Ser-123 in the binding of substrate had been proposed, primarily from the structure in the crystal of RNase S-inhibitor complexes (Wyckoff and Richards, 1971). When Phe-120 was replaced by leucine, the activity against cytidine cyclic 2',3'-phosphate of the resulting complex was 13% of that seen with the phenylalanine-containing structure (Lin *et al.*, 1972). The Michaelis constants at pH 6.0 for this substrate were not significantly different for the two enzymes, indicating that reduced substrate binding was not responsible for the lowered activity. When alanine replaced Phe-120, only 0.8% of the original activity remained, and binding between the two chains was greatly reduced (Hodges and Merrifield, 1974); in this case, no further delineation of kinetic parameters was reported. On the other hand, when tyrosine replaced Phe-120, activity toward RNA or cytidine cyclic 2',3'-phosphate was unchanged; but the rate of hydrolysis of uridine cyclic 2',3'-phosphate was enhanced almost 2-fold (Hodges and Merrifield, 1974).

When Asp-121 was replaced by asparagine, the k_{cat} of the resulting analog against cytidine cyclic 2',3'-phosphate was 2% of that exhibited by the fully active aspartic acid-containing structure (Stern and Doscher, 1984).

The function of Ser-123 was examined by replacing it with alanine (Hodges and Merrifield, 1975). This modification eliminated any possibility of hydrogen bond formation between this residue and a proton of the amino group at position 4 of the cytosine ring in cytidine cyclic 2',3'-phosphate or the carbonyl oxygen at position 4 of the uracil ring in uridine cyclic 2',3'-phosphate. The expectation that substrate binding might be sharply lowered in the Ala-123 derivative was not realized, however, as it had full activity toward the cytidine substrate and 25% activity toward the uridine substrate.

We undertook the crystallographic analysis of RNase 1–118·111–124 to learn how the synthetic tetradecapeptide overlapped RNase 1–118 to achieve full activity in the complex and to establish a structural basis for interpreting the somewhat puzzling kinetic properties of the analogs discussed above. In this report, we present the refined structure at 1.8 Å of the parent semisynthetic molecule in crystals grown from ammonium sulfate/cesium chloride solutions at pH 5.2.

EXPERIMENTAL PROCEDURES

Crystallization—RNase 1–118 and RNase 111–124 were prepared as previously described (Doscher *et al.*, 1983a). Crystals were grown from a 3.0 M CsCl, 1.3 M ammonium sulfate solution at pH 5.2 (Sasaki

[1] The abbreviations used are: RNase A, bovine pancreatic ribonuclease A; RNase S, noncovalent complex of residues 1–20 and 21–124 formed by limited subtilisin digestion of RNase A; RNase 1–118, polypeptide composed of residues 1–118 of RNase A; RNase 111–124, tetradecapeptide composed of residues 111–124 of RNase A; RNase 1–118·111–124, noncovalent complex of RNase 1–118 and RNase 111–124.

et al., 1979a) in space group P3$_2$21 with one molecule in the asymmetric unit and unit cell dimensions $a = b = 67.68$ Å, $c = 65.01$ Å, $\gamma = 120°$ (Doscher *et al.*, 1983b).

Data Collection—CsCl was removed by transferring the crystals directly into a stabilizing buffer of 80% saturated ammonium sulfate, 0.1 M ammonium acetate, pH 5.2. Individual crystals were soaked between 24 and 48 h, with several changes of the solution, before being mounted in a glass capillary in the usual manner. The crystals deteriorated noticeably if stored much longer in the absence of CsCl. Data were collected on a Nicolet P2(1) four-circle diffractometer using an 11-step ω scan of 0.33° at 0.66°/min, and the seven highest consecutive values were retained as the intensity measurement. The nickel-filtered copper x-rays were generated at 40 kV and 26 mA. An empirical curve, which was measured as a function of two θ and ϕ, was used to correct for background. Radiation damage, which was less than 10%, was corrected by the method of Fletterick *et al.* (1976); and the absorption correction was calculated by the method of North *et al.* (1968).

RESULTS

The data to 2.0-Å resolution were collected from one crystal in two shells of resolution. The data from 2.5 to 2.0 Å were collected first, followed by the data from 10 to 2.5 Å. Of the 6280 possible reflections in the 10–2.5-Å shell, 5824 (93%) were observed at better than twice $\sigma(I)$, based on counting statistics. The same statistic for the 2.0–2.5-Å shell was 5055 of 5857, or 86%. R(sym) for the 176 $hk0$ and $kh0$ reflections related by symmetry, which were automatically collected as part of the asymmetric unit, was 0.037.

Later in the project, higher resolution data were collected from 2.3 to 1.8 Å on a second crystal. Friedel pairs were collected, the better to estimate these weaker data. Of the 8,542 possible reflections in the shell, 4,828 (57%) were observed with I > 2*$\sigma(I)$, indicating that 1.8 Å is the practical diffraction limit of these crystals. The Friedel R-factor was 0.093 for these reflections. The data were merged with those obtained from the first crystal, using some 3,888 overlaps in the range 2.3–2.0 Å (merging R-factor = 0.116). The final data set contained 12,117 reflections with intensities greater than twice their standard deviations out of a possible 16,590 reflections in the 10–1.8-Å shell.

Rotation Search—We solved the structure of RNase 1–118·111–124 using the molecular replacement method (Rossmann and Blow, 1962; Lattman and Love, 1970) with the refined alcohol form of RNase A as the model (Wlodawer and Sjolin, 1983). The programs were originally written by E. E. Lattman, Johns Hopkins University, and were modified to run on a VAX 11/780 computer. Coordinates from the Protein Data Bank (Brookhaven National Laboratory, Upton, NY, File 4RSA) were first rotated into a RNase S coordinate system that had been used in earlier low resolution work (Sasaki et al., 1979b) using a least-squares procedure. The equations for transforming the coordinates to the RNase S system were: $X' = 0.13253\ X + 0.05382\ Y - 0.98972\ Z - 1.77182$; $Y' = -0.95575\ X - 0.25756\ Y + 0.96474\ Z - 2.22688$; and $Z' = -0.26264\ X + 0.96474\ Y + 0.01729\ Z - 3.01720$.

For the rotation and translation searches, the transformed RNase A coordinates were initially placed with the center of mass at the origin of a 100-Å P1 orthogonal unit cell. The rotational asymmetric unit in space group Pbn2(1), which is defined by the limits of 0–120 on θ_1, 0–90 on θ_2, 0–360 on θ_3, 0–720 on $\theta+$, and 0–120 on $\theta-$ (Tollin *et al.*, 1966; Rao *et al.*, 1980), was searched in $\theta+/\theta-$ space (Lattman, 1972) with the highest 20% of the data on a coarse grid of 15° at 4-Å resolution. Fig. 1 shows the section at $\theta_2 = 75$. The peak at $\theta- = 120$, and $\theta+ = 414$ is 5.8 δ, as defined by Lattman *et al.* (1971), above the average value of the map and 2.5 δ above the next highest peak. A symmetry-related peak was found at $\theta- = 0$ and $\theta+ = 288$. Fine scans at 3 Å in 5° increments and
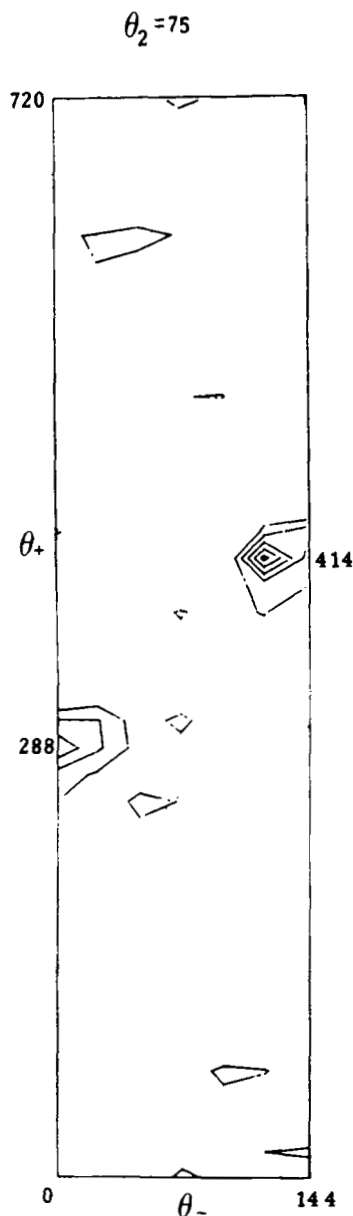

FIG. 1. **The only section ($\theta = 75°$) of the rotation function having significant peaks.** The highest 20% of the data between 10- and 4-Å resolution were used in the calculation. The peaks at $\theta+ = 0$, $\theta- = 288$ and at $\theta+ = 120$, $\theta- = 414$ are related by symmetry.

at 2.5 Å in 1° increments, again using only the highest 20% of the data, around the peak at $\theta- = 0$ and $\theta+ = 288$ produced the final rotation angles of $\theta_1 = 145.75$, $\theta_2 = 76.4$, and $\theta_3 = 148.75$.

Translation Search—The translation search (Rossmann and Blow, 1964; Crowther and Blow, 1967) used all of the data to 2-Å resolution. A search for the vector between the molecule at x,y,z and the symmetry mate at $y-x,-x,\frac{1}{3}+z$ produced a single peak at $u = 0.325$, $v = 0.225$, and $w = \frac{1}{3}$. Likewise, the vectors between molecules at x,y,z and $-y,x-y,\frac{2}{3}+z$ produced a single peak at $u = 0.250$, $v = 0.900$, and $w = \frac{2}{3}$, consistent with the $w = \frac{1}{3}$ section. Finally, a search for the vectors between molecules at x,y,z and $y,x,-z$ over the entire unit cell produced a peak at $u = 0.812$, $v = 0.188$, and $w = 0.150$. All these peaks, each of which was at least 6 standard deviations above the mean value of the map, were essentially the only ones seen in the translation. These results, taken together, form a self-consistent solution to the trans-

lation problem, placing the local origin of the molecule at $x = 0.475$, $y = 0.290$, which are the average values for independent solutions on the two Harker sections, and $z = 0.425$. They also identify the space group as $P3_221$ and not the enantiomorph (Schmid *et al.*, 1974).

Refinement—The rotation angles $\theta_1 = 25.75$, $\theta_2 = 76.4$, and $\theta_3 = 148.75$, which were picked arbitrarily for the molecule at *x,y,z* in the translation search, and the translation vector gave us a starting set of coordinates for the refinement. We were concerned that using a phase set derived from a known structure could seriously bias the structure we wished to determine. We therefore removed residues 111–124, which were the most likely to differ from the model, from the RNase coordinate list before we calculated the initial phases. The refinement was started (Table I, step 3) using a rigid body least-squares program written by W. Hendrickson, Columbia University. Using all the data from 10 to 2 Å, six cycles reduced the *R*-factor from 0.420 to 0.363. The rotation angles θ_1, θ_2, and θ_3 changed by $+0.01°$, $-0.07°$, and $+0.89°$, respectively, and the *x,y,z* coordinates of the local origin changed by $+0.18$, $+0.13$, and $+0.06$ Å, respectively. An F_o-F_c map revealed the positions of residues 114–124, shown in Fig. 2, and confirmed that enough information was contained in our amplitudes to warrant a complete least-squares refinement of the semisynthetic enzyme. The positions of residues 111–118 in the protein and residues 111–113 in the synthetic fragment were not apparent at this time, presumably because either they were too disordered or the phase set was not yet good enough to reveal them.

The side chains of residues that have been implicated in the catalytic mechanism of RNase, namely, Lys-7, His-12, Lys-41, His-119, Phe-120, and Asp-121, were removed from the coordinate list. Refinement was started at 2.5-Å resolution (Table I, step 4) and continued for nine cycles. Then, data to 2.0 Å were added, and the refinement was continued for another five cycles. An F_o-F_c map placed the side chain atoms unambiguously for all the excluded residues, except His-119, for which there was some density in the B position reported by Borkakoti *et al.* (1982); the earlier F_o-F_c map at $R = 0.36$

had shown density at both the A and the B positions.

In view of the crucial role of His-119 in the catalytic mechanism, we decided to extend the resolution of the model to 1.8 Å with the hope of obtaining a clearer view of this residue. The refinement (Table I, step 6) was continued with the higher resolution data for an additional four cycles, and a $2F_o$-F_c map was calculated. All the side chain atoms that had been left out, except His-119, were fitted at this point and added to the coordinate list. It was reassuring that we could see the Lys-41 side chain so clearly (Fig. 3) in view of the problems encountered with this residue in previous structure determinations of both RNase A and S. Reasonable density for Gly-112 in RNase 1–118 also appeared at this point. A strong peak in the active site was assigned to a sulfate ion based upon a difference electron density map that had been calculated from diffraction data collected on RNase A crystals in 3.8 M ammonium sulfate at pH 6 and 9 (Martin, 1978). A difference map calculated after a further five cycles of refinement (Table I, step 7) contained well-defined density for His-119 (Fig. 4). This residue was added to the coordinate list, and refinement was continued for an additional three cycles to an *R*-value of 0.251.

A real space search program was then used to find the positions of putative water molecules in F_o-F_c difference electron density maps. The refinement was stopped intermittently for graphics intervention to see that the waters we were including not only remained in reasonable positions, but had significant density at the positions they refined to. We found that by the end of step 9 (Table I), the data from 7 to 10 Å were very poorly estimated by the structure, even with the inclusion of some 45 water molecules. These data were subsequently left out of the refinement. Typically, the addition of water positions was followed by four to six cycles of refinement in which positions and temperature factors were allowed to vary until they converged. This was followed by an additional four to six cycles of refinement allowing occupancies to vary. The structure was then observed on the graphics system to check the current addition of water. At cycle 56, we changed the orientation of residue 89, as discussed by Wlo-

TABLE I

Summary of the structure refinement

Step	Program[a]	Data	Cycles	Protein residues omitted[b]	Peptide residues omitted[b]	R-factor[c]
		Å				
1	Rotation search	10–4		None	111–124	
		10–3		None	111–124	
		10–2.5		None	111–124	
2	Translation search	10–2		None	111–124	0.42
3	Rigid body least-squares	10–2	6	111–124	111–124	0.363
4	RLS[d]	10–2.5	9	7*, 12*, 41*, 111–118	111–113, 114*, 119*, 120*, 121*	0.264
5	RLS	10–2	5	7*, 12*, 41*, 111–118	111–113, 114*, 119*, 120*, 121*	0.259
6	RLS	10–1.8	4	7*, 12*, 41*, 111–118	111–113, 114*, 119*, 120*, 121*	0.271
7	RLS	10–1.8	5	111–118[e]	111–113, 114*, 119*	0.253
8	RLS	10–1.8	3	113–118	111–113, 114*	0.251
9	RLS	10–1.8	17	113–118[f]	111–113, 114*	0.236
10	RLS	7–1.8	57	114–118[g]	111–113	0.204

[a] The rotation and translation search programs were written by E. E. Lattman; the rigid body and restrained least-squares programs were written by W. Hendrickson.
[b] Residues where only the side chain atoms beyond the C_β were omitted are indicated by asterisks.
[c] R factor $= (\sum \| F_o \| - \| F_c \|)/\sum | F_o |$.
[d] RLS, restrained least-squares program. Individual temperature factors were included from this step onward.
[e] A sulfate ion was placed in the active site.
[f] Forty-five water molecules were included in the last four cycles of refinement.
[g] One-hundred and five water molecules were included in the last four cycles of refinement.

FIG. 2. **Stereo photograph of residues 114–124 in a F_o-F_c map calculated after step 3 (Table I).** None of the atoms was included in the rigid body refinement or phase calculation. His-119 is shown in the A (*upper*) and B (*lower*) positions. Positive contours are at twice the root mean square fluctuation in featureless sections of the map.
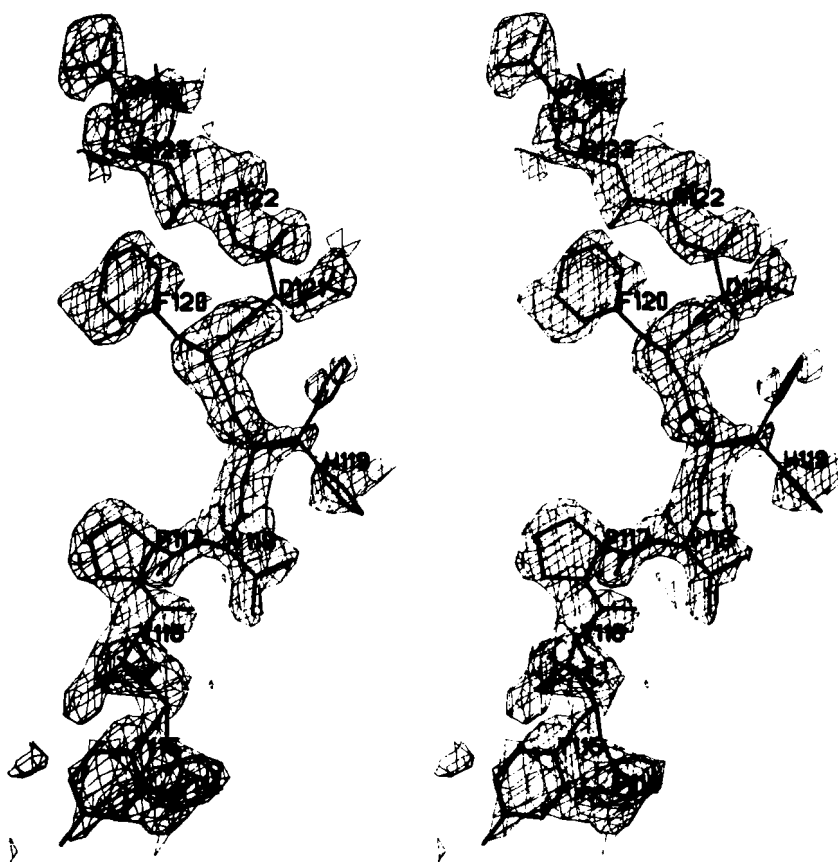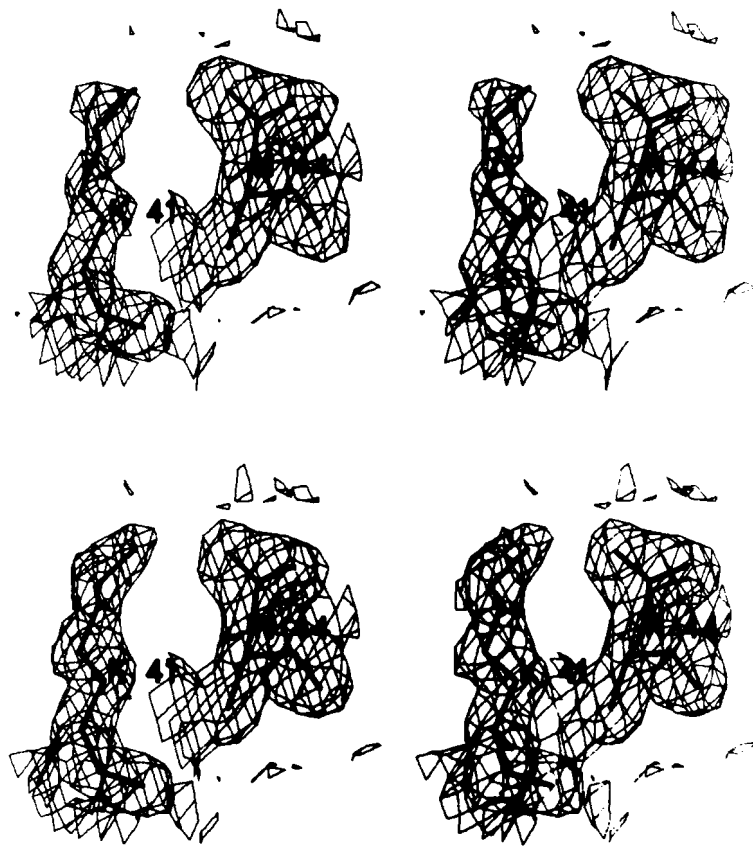
FIG. 3. **Stereo photographs of Lys-41 and Asn-44 fitted to a F_o-F_c map calculated after step 6 (*upper*) or step 9 (*lower*).** Atoms beyond C_β were not included in the refinement or phase calculation for the *upper*. Both maps were contoured as described for Fig. 2.
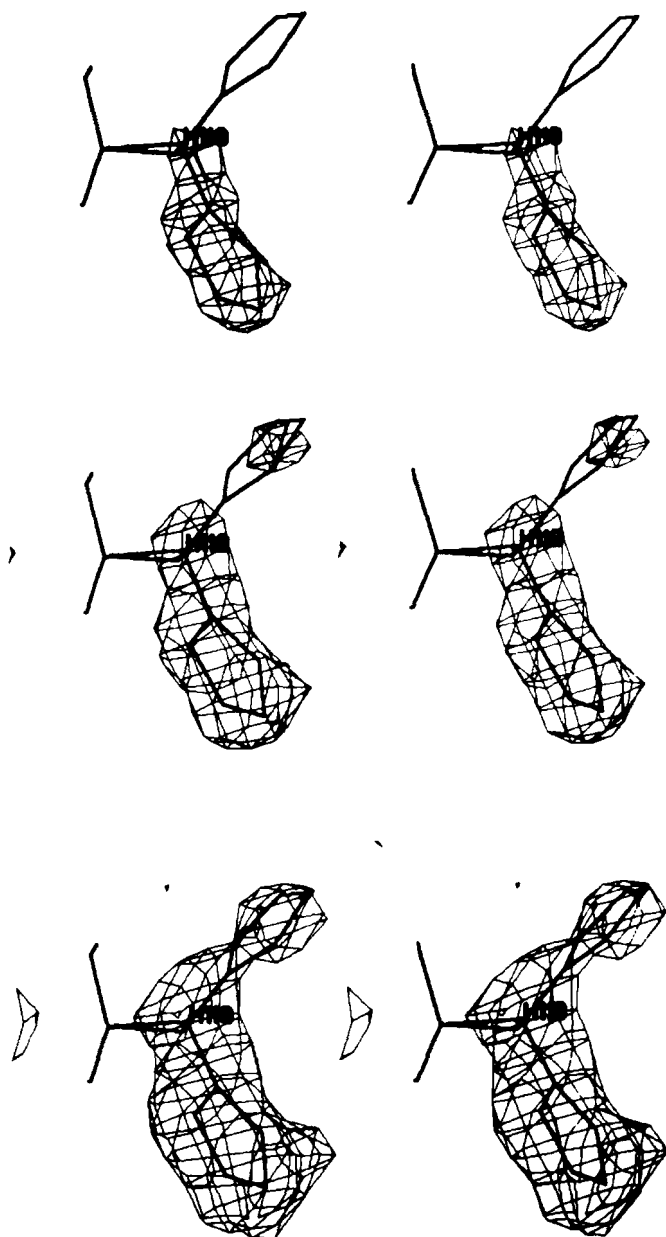
1.8-Å Crystal Structure of a Semisynthetic Ribonuclease

FIG. 4. F_o-F_c **difference electron density maps for His-119 in the A (*upper*) and B (*lower*) positions.** None of the atoms shown was included in the phase calculation. All panels are contoured after cycle 102. From *bottom* to *top*, maps are shown at the two, three, and four σ levels.

dawer *et al.* (1986), to that of Borkakoti *et al.* (1982) because the density clearly showed this to be the better choice. Throughout the refinement, AFSIG and BFSIG, essentially the only parameters adjusted throughout the refinement, were kept at values such that the root mean square deviation from ideal bond distances remained around 0.025 Å. A total of 105 water molecules were finally added to the structure. The final *R*-value is 0.204. The root mean square deviation of bond lengths from ideality in the final model is 0.024 Å and that of planar groups is 0.010 Å.

DISCUSSION

RNase 1–118 Main Chain Atoms—Most of the backbone structure of RNase 1–118·111–124 closely resembles that observed in crystals of RNase A. A tabulation of some previous x-ray and neutron diffraction studies of RNase appears in

Table II. The root mean square deviation of the C_α positions of residues 1–112 is 0.37 Å with respect to the coordinates reported by Wlodawer and Sjolin (1983) (Brookhaven File 4RSA) and 0.42 Å with respect to those of Borkakoti *et al.* (1982) (Brookhaven File 1RN3). The last 5 residues of RNase 1–118 are not seen in our map. When these values are compared with the root mean square difference between the alcohol forms of 0.11 Å in the main chain (Wlodawer *et al.*, 1986), it suggests that there are small, but real differences between our model and these structures. The root mean square deviations from the coordinates of Wlodawer and Sjolin (1983) and from those of Borkakoti *et al.* (1982) of residues 114–124 in the tetradecapeptide are 0.68 and 0.69 Å, respectively. The larger differences are not unexpected, given the noncovalent binding of these residues to RNase 1–118.

The backbone hydrogen bonding observed in RNase 1–118·111–124 (Fig. 5) closely resembles the refined RNase A structures already reported (Wlodawer and Sjolin, 1983; Borkakoti *et al.*, 1982). The hydrogen atoms were attached with ideal geometry and then used to calculate hydrogen bond angles and distances. A noteworthy feature is the near identity between the intramolecular backbone bonding pattern seen at the C terminus in RNase A and the intermolecular pattern seen between RNase 1–118 and the tetradecapeptide in our model. Of the seven "short" and two "long" bonds reported for this region by Wlodawer and Sjolin (1983), only the long bond from His-119 to Ala-109 is absent in our structure. (Borkakoti *et al.* (1982) report only the seven short bonds in this region.) Evidently, the noncovalent interactions between the two chains result in a structure almost precisely the same as that formed by the intact chain. The only novel interaction seen in our model in this region is a short hydrogen bond from Asn-113 in the protein to Pro-114 in the peptide (Fig. 5). We see all the remaining backbone hydrogen bonds reported by Wlodawer and Sjolin (1983), but the direction of the Val(63)-Cys(72) bond is reversed in our model. In addition, we find bonds from Lys-41 to Leu-35 (short), from Lys-61 to Gln-74 (long), and from Ser-90 to Thr-87 (long). The presence of the bond between Lys-41 and Leu-35 may be related to the clarity with which we see the side chain of Lys-41 (see below).

Histidine 12—In concurrence with all previous structural studies on RNase (Wyckoff *et al.*, 1970; Wlodawer and Sjolin, 1982, 1983; Borkakoti et al., 1982), we find His-12 to be in good density and in a position to form a long hydrogen bond with an oxygen of the sulfate molecule at the active site.

Lysine 41—Although earlier reports indicated that Lys-41 was positioned too far from the active site to be an effective participant in catalysis (Richards and Wyckoff, 1973; Wlodawer and Sjolin, 1982), more recent work has modified this view. Borkakoti *et al.* (1982) place nitrogen NZ of Lys-41 6.8 Å from the sulfur atom of the active site sulfate and postulate hydrogen bonding linkage to an oxygen atom of the sulfate via a bridging water molecule. This same water molecule forms a third hydrogen bond to the carbonyl OD of Asn-44. The inclusion of neutron diffraction data with their x-ray diffraction results caused Wlodawer and Sjolin (1983) to reposition the Lys-41 side chain in a way that brought it within 3.02 Å of an oxygen atom of the phosphate ion that is found at the active site in their structure and within 2.94 Å of the side chain oxygen of Asn-44 (Borah *et al.*, 1985). In our model of RNase 1–118·111–124, the side chain of Lys-41, which has an average *B* value of 24.9 Å², is clearly seen with the nitrogen NZ in a position to hydrogen bond directly to the carbonyl OD of Asn-44 (distance from NZ to OD = 2.74 Å and the angle NZ-HZ2-OD = 142°), to the side chain carbonyl oxygen

TABLE II

Some previous x-ray and neutron diffraction studies of bovine pancreatic ribonuclease

For a recent review of this area, see Wlodawer (1984).

| RNase species	Crystal Environment		Space group and unit cell dimensions	Radiation	Resolution	R-factor	Ref.
	pH	Solvent					
					$\mathring{A}$		
A	5.25	55% deuterated t-butyl alcohol (d_{10}), 45% D_2O (99.8%)	$P2_1$; $a = 30.2$, $b = 38.4$, $c = 53.3$, $\beta = 105.8°$	X-ray; neutron	2.0	0.159 (x-ray), 0.183 (neutron)	Wlodawer and Sjolin (1983)
A	5.2–5.7	60% aqueous ethanol	$P2_1$; $a = 30.4$, $b = 38.4$, $c = 53.2$; $\beta = 106°$	X-ray	1.45	0.26	Borkakoti et al. (1982)
S	5.5	75% saturated $(NH_4)_2SO_4$ (0.1 M acetate)	$P3_121$; $a = b = 44.6$, $c = 97.2$	X-ray	2.0	Not refined	Wyckoff et al. (1970)
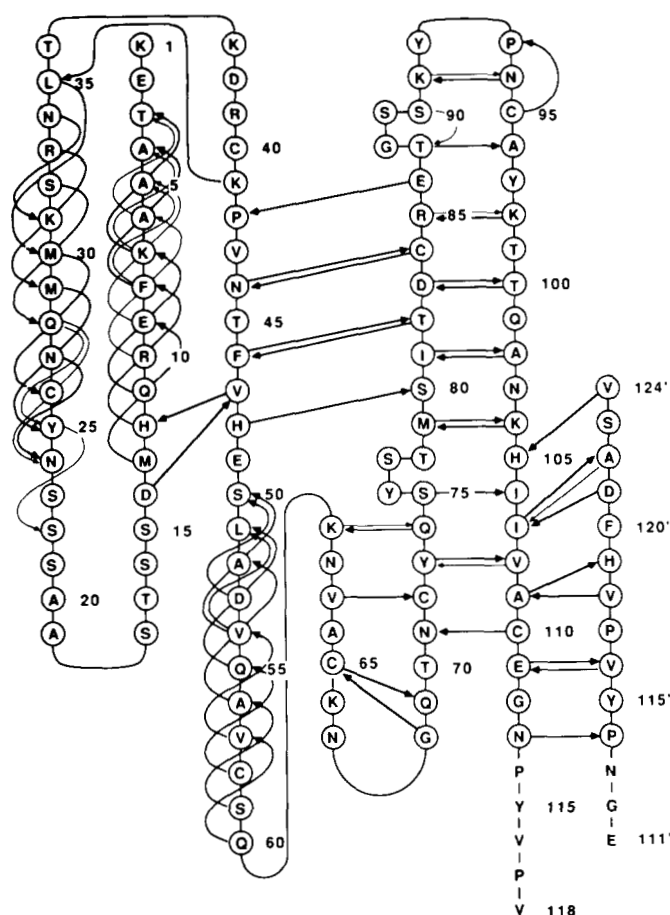
FIG. 5. **Backbone hydrogen bonding scheme for RNase 1–118•111–124.** Hydrogens were affixed in ideal positions for the calculation of the hydrogen bond angle, which was required to be greater than 110°. The *thicker lines* represent short hydrogen bonds between 2.5 and 3.15 Å; the *thinner lines* represent long hydrogen bonds between 3.15 and 3.35 Å.

of Gln-11 (NZ to OE1 = 3.12 Å and NZ-HZ1-OE1 = 169°), and to a water (NZ to O = 2.72 Å) (Fig. 3).

Still more recently, Wlodawer et al. (1983) and Borah et al. (1985) have determined the active site structure of RNase A in the presence of uridine vanadate, a transition state analog (Lindquist et al., 1973). Under these conditions, the side chain amino group of Lys-41 forms two strong hydrogen bonds, the

first to the side chain of Asn-44 (distance from NZ to OD = 2.77 Å and the angle NZ-DZ2-OD = 161°) and the second to the apical O2′ oxygen of the ribose moiety of the uridine (distance from NZ to O2′ = 2.76 Å and the angle NZ-DZ2-O2′ = 174°). Almost all previous structural, kinetic, NMR, and theoretical studies had assigned the role of interacting with the apical O2′ oxygen to His-12 (Richards and Wyckoff, 1973; Blackburn and Moore, 1982). Evidence for an interaction between Lys-41 and the 2′-hydroxyl moiety of the ribose ring of several mononucleotide inhibitors has been presented, however, by Jentoft et al. (1981) in their study of the ^{13}C NMR spectra of ^{13}C-methylated RNase A.

Peptide 111–124 Main Chain Atoms—We found excellent agreement between the positioning of many of the main chain atoms in the tetradecapeptide and those in the corresponding part of the RNase A chain as seen by Wlodawer and Sjolin (1983) (Fig. 6). On the other hand, as discussed fully below, the side chain positioning of His-119 differed from that seen by Wlodawer et al. (1983) and Borah et al. (1985).

To delineate the structural elements responsible for the generation of enzymatic activity upon the binding of the tetradecapeptide to RNase 1–118, Gutte et al. (1972) measured the activity of complexes between RNase 1–118 and a series of shorter peptides. The activities were measured at saturating mole ratios of peptide to RNase 1–118 and were reported as maximal regenerable activity against cytidine cyclic 2′,3′-phosphate relative to that of an equimolar amount of RNase A. The complex between RNase 1–118 and the heptapeptide comprised of residues 118–124 exhibited a maximum of 1% activity, whereas the activities of complexes with successively longer peptides were 1.5% (117–124), 60% (116–124), 70% (115–124), and 90% (113–124). As saturating levels of the peptide moiety were used in each case, the striking increase in the activity of the complex upon the addition of Val-116 to the synthetic fragment must correspond to an increased catalytic efficiency (k_{cat}/K_M) of the active site and not to any such differences in strength of binding to RNase 1–118 as may exist among the peptides tested. The pattern of interchain hydrogen bonding which we see between RNase 1–118 and the tetradecapeptide (Fig. 5) suggests why the presence of Val-116 in the peptide is so important for the formation of an effective active site. In the absence of this residue, which forms two good interchain backbone hydrogen bonds with Glu-111, there is no hindrance to the formation of the same two intrachain hydrogen bonds by the Val-116 of RNase 1–118, *i.e.* the structure found in RNase A. This latter struc-
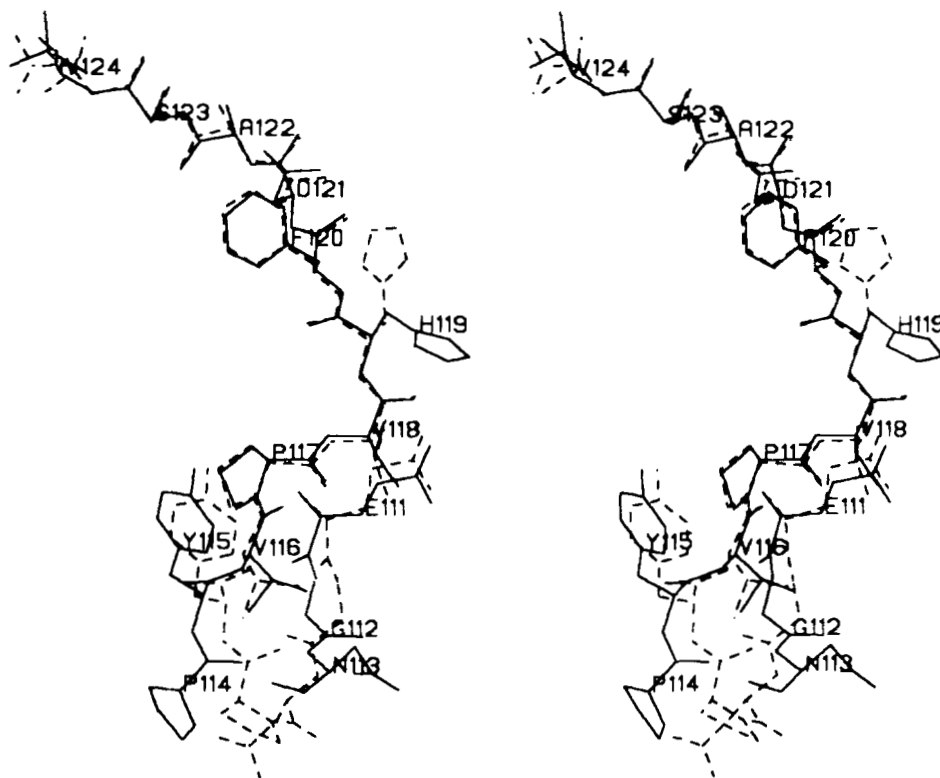
FIG. 6. **Stereo photograph of residues 111–124 of the Wlodawer and Sjolin (1983) structure (*dashed*) and our structure overlapped by a least-squares procedure in which only the backbone C_α atoms of residues 1–110 were used in the overlap.** Only the area around the break in the chain and the side chain of His-119 (see text and Fig. 4) were significantly different from the RNase A structure in this part of the molecule.

ture would place the C-terminal Val-118 of RNase 1–118, which can form its own hydrogen bond to Ala-109, within a few angstroms of the peptide His-119, a situation likely to disturb elements of the active site such as its polarity, geometry, or rigidity.

Gutte *et al.* (1972) also observed progressive and comparable increases in the activity of the semisynthetic complex when Tyr-115, Pro-114, Asn-113 and the Glu-Gly sequence at positions 111–112 were included as part of the synthetic peptide. Moreover, the binding energy between the two chains increases significantly upon the addition of these 5 residues, with the K_D of the complex between RNase 1–118 and RNase 116–124 at pH 6.0 being 2.5 μM; whereas the value for RNase 1–118 and RNase 111–124 is 0.2 μM. The initial difference map showed no density beyond Pro-114 for the peptide, but Pro-114 and Tyr-115 could be fitted as shown in Fig. 2. During step 10 of the refinement, however, it became apparent that the positioning of these residues was incorrect; so they were refitted, and, in addition, the Asn-113 of the protein was inserted. These operations revealed the presence of a novel hydrogen bond between this Asn-113 and the Pro-114 of the peptide (Fig. 5). No interpretable density was seen for residues 111–113 of the peptide or residues 114–118 of the protein. If the hydrogen bond between Asn-113 of the protein and Pro-114 of the peptide exists in solution, it could explain some, but not all, of the effects of lengthening the peptide beyond Val-116. Any remaining discrepancies may reflect the fact that the solution data were all obtained in the presence of substrate, whereas the crystal data were not.

Histidine 119—Borkakoti *et al.* (1982) have reported that for crystals of RNase A grown from 60% aqueous ethanol (Table II), active site residue His-119 occupies two discrete locations, labeled positions A and B. The former has torsion angles[2] $\chi_1 = 149°$ and $\chi_2 = 106°$ and an occupancy of 0.80,

compared with torsion angles $\chi_1 = -76°$ and $\chi_2 = -55°$ and an occupancy of 0.20 for position B. In position A, nitrogen atom ND1 of the imidazole ring is within hydrogen bonding distance of one of the oxygen atoms of the sulfate that is found at the active site in these crystals. In position B, achieved by rotation about the C_α-C_β bond, the distances from the imidazole ring to both the sulfate and the His-12 side chain are increased several angstroms over those seen in position A. In the unrefined RNase S structure, which was determined with crystals in aqueous ammonium sulfate, Wyckoff *et al.* (1970) had earlier found that His-119 occupied several discrete positions. Wlodawer and Sjolin (1983) and Wlodawer *et al.* (1982), working with crystals of RNase A in 55% aqueous *t*-butyl alcohol, have reported only one position for His-119, which has side chain torsion angles of 143° and 89°, *i.e.* essentially those of position A as defined by Borkakoti *et al.* (1982). However, in crystals of RNase 1–118·111–124, which are in 80% saturated ammonium sulfate, the major electron density for His-119 (Fig. 4) is in position B, with side chain torsion angles of $\chi_1 = -47°$ and $\chi_2 = -66°$. In this position, the ND1 nitrogen forms a hydrogen bond with an oxygen of the sulfate in the active site, but not the same oxygen that is involved when His-119 is in position A.

At the end of the refinement, His-119 and a "water" that had been found in the A position were removed from the coordinate list, four cycles of refinement were performed, and a difference map was calculated. Maps at the two, three, and four σ levels are shown in Fig. 4. Clearly, the major occupancy is at position B, with significant, but distinctly less, density appearing at position A. Thus, in our structure, His-119 occupies predominantly the position seen as a minor site by Borkakoti *et al.* (1982) and not at all by Wlodawer and Sjolin (1983).

No consequences of the varying His-119 position seen in the crystalline state are manifest in the C-2 proton NMR spectra of the 4 histidine residues in the molecule, the data for RNase 1–118·111–124 being identical with those for

[2] Torsion angles for the various His-119 side chain positions in structures reported from other laboratories were calculated by us using coordinates filed in the Protein Data Bank, Brookhaven National Laboratory, Upton, NY.

RNase A (Doscher *et al.*, 1983a). If the rate of interconversion between the two conformations were sufficiently rapid, however, no NMR spectral detection would be expected.

The possibility of positioning His-119 in two conformations of apparently comparable energy is provocative in view of the fact that RNase catalyzes two distinct reactions: first, a transphosphorylation that cleaves the RNA chain and results in the formation of a cyclic 2',3'-phosphate ester at the terminus of the 3' portion of the original chain; and second, the hydrolysis of this cyclic ester to a 3'-phosphate monoester. It might be noted that many studies of the mechanism of action of the enzyme have focused exclusively on either the first reaction (Holmes *et al.*, 1978; Deakyne and Allen, 1979) or the second one (Findlay *et al.*, 1962), thus tending to obscure the difficulty of having the same active site geometry catalyze two different reactions.

Temperature Factors—Temperature factors, or *B*-values when measured in squared angstroms, include the effects of thermal mobility and static disorder (Artymiuk *et al.*, 1979; Frauenfelder *et al.*, 1979). For simplicity, we shall discuss them as measures of mobility, although our data do not separate the two effects. The average temperature factor of 19 Å^2 for the main chain atoms in our model is higher than the average values of 10 and 14 Å^2 for the models of Wlodawer and Sjolin (1983) and Borkakoti *et al.* (1982), respectively. These differences are not unexpected, given the fact that the RNase A crystals grown from alcohol diffract to higher resolution. The six largest maxima in Fig. 7A, which occur at residues 1, 21, 38, 69, 92, and 114, indicate regions of exceptional mobility in our model.

To facilitate comparison among the thermal factors of the three models, we used the mean and standard deviation of each set to convert the average *B*-values for each residue to
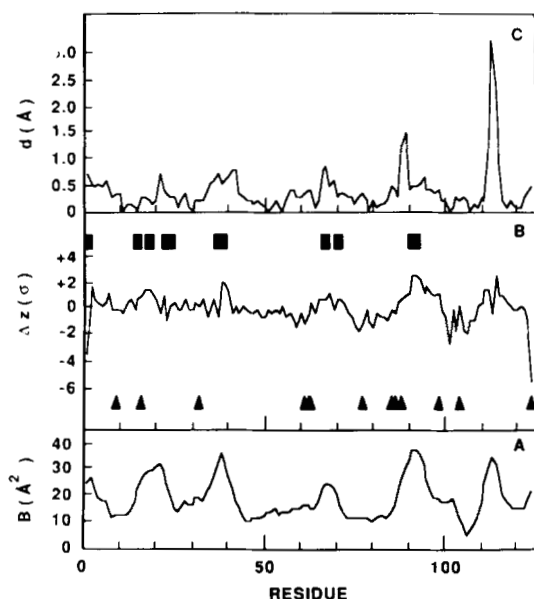

FIG. 7. **Mobility of the backbone atoms.** *A*, average temperature factors for the main chain atoms of RNase 1–118·111–124. *B*, the average main chain temperature factor for each residue in RNase A (Borkakoti *et al.*, 1982) expressed in terms of a standard deviation, that is, as a *Z*-value (see text) and subtracted from the *Z*-value of the same residue in RNase 1–118·111–124. The residues marked by a *triangle* below the curve are involved in intermolecular hydrogen bonds in the RNase 1–118·111–124 crystals, whereas those marked by a *square* above the curve are similarly involved in the RNase A structure. *C*, the difference between the positions of the C$_\alpha$ atoms in RNase 1–118·111–124 and in RNase A (Borkakoti *et al.*, 1982) after the two structures had been superimposed by a least-squares method.

Z-values, that is, the number of standard deviations that the *B*-value is above or below the average *B*-value for its model. Fig. 7B shows the difference between the *Z*-values for our model and those of Borkakoti *et al.* (1982). The regions centered at residues 39, 91, and 114 are relatively more mobile by 1.5 S.D. in our model, whereas the regions around residues 1, 76, 101, and 124 are relatively less mobile by 1.5 S.D. Some of these differences can be rationalized by differences in packing between the RNase A crystals grown from alcohol and our crystals grown from ammonium sulfate. In our crystals, there are fewer intermolecular contacts around residues 39 and 91; consequently, it is reasonable that these regions should be more mobile. Conversely, the regions around residues 76, 101, and 124 have more intermolecular contacts in our model. Exceptions to this explanation occur at residues 1 and 114. Our model is relatively less mobile at the N terminus, although it lacks the intermolecular contact present in the model of Borkakoti *et al.* (1982). The mobility of the main chain around residue 114, where neither model has intermolecular contacts, is higher in our model because that is where the separation between the two pieces of RNase 1–118·111–124 occurs.

Fig. 7C reveals that the two largest differences in the positions of the C$_\alpha$ atoms occur at residues 89 and 114 when our model is overlapped in a least-squares sense with that of Borkakoti *et al.* (1982). Again, the latter difference can be explained by the presence of the separation between the two pieces of RNase 1–118·111–124. The precise cause of the displacement at residue 89 is unclear. Our model has an additional hydrogen bond from Ser-90 to Thr-87. Also, this region has the highest temperature factors in our model.

Bound Water—Our model includes 105 water molecules. Twenty-nine of these are located within 1 Å of waters seen by Wlodawer and Sjolin (1983), whereas the corresponding number of overlaps with the model of Borkakoti *et al.* (1982) is nine. Eight water molecules were found to coincide in all three maps. In contrast, a comparison of the two independently refined structures of RNase A from alcohol (Wlodawer *et al.*, 1986) places 58 of the 128 and 123 waters seen in the two models within 1 Å of each other. In view of the similarity in the positioning of the C$_\alpha$ atoms in our model and in the alcohol structures (root mean square deviations of 0.39 and 0.44 for the structures of Wlodawer *et al.* (1986) and Borkakoti *et al.* (1982), respectively), these differences in water structure would appear to reflect primarily the great differences in ionic strength and dielectric constant of the crystallization media.

The hydrogen bonding interactions of the three water molecules which we see at the active site are shown in Fig. 8. Of these three, only one is common to the three refined structures; it is within hydrogen bonding distance of NE2 of Gln-11 and two sulfate oxygens. As calculated by least-squares overlap from the appropriate main chain coordinates, our sulfur atom is 0.15 Å from the sulfur position reported by Borkakoti *et al.* (1982) and 0.25 Å from the phosphorus position reported by Wlodawer and Sjolin (1983); these two latter positions differ by 0.38 Å.

Neither the overall structure nor the active site details of RNase 1–118·111–124 so far provide a clue about the puzzling kinetic properties exhibited by several structural analogs of this molecule. Further crystallographic examination of the active site in the presence of such ligands as uridine vanadate (Lindquist *et al.*, 1973; Wlodawer *et al.*, 1983; Borah *et al.*, 1985), UpcA (Richards and Wyckoff, 1973), and 2'-deoxy-2'-fluorouridilyl-3',5'-adenosine (Pavlovsky *et al.*, 1978) may provide useful information. A more telling line of investigation, however, is likely to be x-ray diffraction analysis of
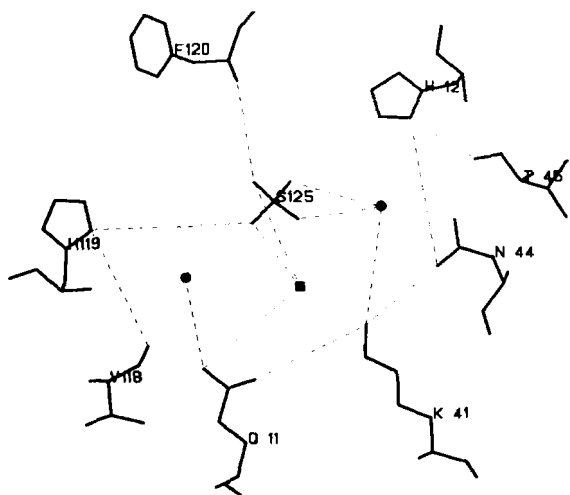
FIG. 8. **Schematic hydrogen bonding scheme of the sulfate (S125) and the three water molecules found in the active site.** Of the three, one (■) is common to all three structures. The two additional waters (●) are unique to our structure, that is, >1 Å from any candidate waters in the other two structures. Hydrogen bonds, indicated by *dashed lines*, all had bond angles greater than 110° and bond lengths shorter than 3.15 Å.

crystals of one or more of the catalytically defective analogs. Diffraction quality crystals of the Leu-120 analog ($k_{cat} = 13\%$ that of the Phe-120 enzyme) and the Asn-121 analog ($k_{cat} = 2\%$) that are isomorphous with the parent enzyme are presently in hand (Doscher et al., 1983b; Stern et al., 1986).

REFERENCES

Artymiuk, P. J., Blake, C. C. F., Grace, D. E. P., Oatley, S. J., Phillips, D. C., and Sternberg, M. J. E. (1979) *Nature* **280**, 563–568

Blackburn, P., and Moore, S. (1982) in *The Enzymes* (Boyer, P. D., ed) 3rd Ed., Vol. 15, pp. 317–433, Academic Press, New York

Borah, B., Chen, C., Egan, W., Miller, M., Wlodawer, A., and Cohen, J. S. (1985) *Biochemistry* **24**, 2058–2067

Borkakoti, N., Moss, D. S., and Palmer, R. A. (1982) *Acta Crystallogr. Sect. B Struct. Crystallogr. Cryst. Chem.* **38**, 2210–2217

Crowther, R. A., and Blow, D. M. (1967) *Acta Crystallogr. Sect. A Cryst. Phys. Diffr. Theor. Gen. Crystallogr.* **23**, 544–548

Deakyne, C. A., and Allen, L. C. (1979) *J. Am. Chem. Soc.* **101**, 3951–3959

Doscher, M. S., Martin, P. D., and Edwards, B. F. P. (1983a) *Biochemistry* **22**, 4125–4131

Doscher, M. S., Martin, P. D., and Edwards, B. F. P. (1983b) *J. Mol. Biol.* **166**, 685–687

Findlay, D., Herries, D. G., Mathias, A. P., Rabin, B. R., and Ross, C. A. (1962) *Biochem. J.* **85**, 152–153

Fletterick, R. J., Sygush, J., Murray, N., Madsen, N. B., and Johnson, L. N. (1976) *J. Mol. Biol.* **103**, 1–13

Frauenfelder, H., Petsko, G., and Tsernoglou, D. (1979) *Nature* **280**, 558–563

Gutte, B., Lin, M. C., Caldi, D. G., and Merrifield, R. B. (1972) *J. Biol. Chem.* **247**, 4763–4767

Hodges, R. S., and Merrifield, R. B. (1974) *Int. J. Pept. Protein Res.* **6**, 397–405

Hodges, R. S., and Merrifield, R. B. (1975) *J. Biol. Chem.* **250**, 1231–1241

Holmes, R. R., Deiters, J. A., and Gallucci, J. C. (1978) *J. Am. Chem. Soc.* **100**, 7393–7402

Jentoft, J. E., Gerken, T. A., Jentoft, N., and Dearborn, D. G. (1981) *J. Biol. Chem.* **256**, 231–236

Lattman, E. E. (1972) *Acta Crystallogr. Sect. B Struct. Crystallogr. Cryst. Chem.* **28**, 1065–1068

Lattman, E. E., and Love, W. E. (1970) *Acta Crystallogr. Sect. B. Struct. Crystallogr. Cryst. Chem.* **26**, 1854–1857

Lattman, E. E., Nockolds, C. E., Kretsinger, R. H., and Love, W. E. (1971) *J. Mol. Biol.* **60**, 271–277

Lin, M. C. (1970) *J. Biol. Chem.* **245**, 6726–6731

Lin, M. C., Gutte, B., Moore, S., and Merrifield, R. B. (1970) *J. Biol. Chem.* **245**, 5169–5170

Lin, M. C., Gutte, B., Caldi, D. G., Moore, S., and Merrifield, R. B. (1972) *J. Biol. Chem.* **247**, 4768–4774

Lindquist, R. N., Lynn, J. L., Jr., and Lienhard, G. E. (1973) *J. Am. Chem. Soc.* **95**, 8762–8768

Martin, P. D. (1978) Ph.D. Dissertation, Wayne State University

North, A. C. T., Phillips, D. C., and Mathews, F. S. (1968) *Acta Crystallogr. Sect. A. Cryst. Phys. Diffr. Theor. Gen. Crystallogr.* **24**, 351–359

Pavlovsky, A. G., Borisova, S. N., Borisov, V. V., Antonov, I. V., and Karpeisky, M. Y. (1978) *FEBS Lett.* **92**, 258–262

Rao, S. N., Jih, J., and Hartsuck, J. A. (1980) *Acta Crystallogr. Sect. A Cryst. Phys. Diffr. Theor. Gen. Crystallogr.* **36**, 878–884

Richards, F. M., and Wyckoff, H. W. (1973) *Atlas of Molecular Structure in Biology: Ribonuclease* Clarendon Press, Oxford

Rossman, M. G., and Blow, D. M. (1962) *Acta Crystallogr. Sect. A. Cryst. Phys. Diffr. Theor. Gen. Crystallogr.* **15**, 24–31

Rossman, M. G., and Blow, D. M. (1964) *Acta Crystallogr. Sect. A Cryst. Phys. Diffr. Theor. Gen. Crystallogr.* **17**, 338–342

Sasaki, D. M., Martin, P. D., Doscher, M. S., and Tsernoglou, D. (1979a) *J. Mol. Biol.* **135**, 301–304

Sasaki, D. M., Martin, P. D., Doscher, M. S., and Tsernoglou, D. (1979b) in *Peptides, Structure and Biological Function* (Gross, E., and Meienhofer, J., eds) pp. 149–151, Pierce Chemical Co. Publishers, Rockford, IL

Schmid, M. F., Herriott, J. R., and Lattman, E. E. (1974) *J. Mol. Biol.* **84**, 97–101

Stern, M. S., and Doscher, M. S. (1984) *FEBS Lett.* **171**, 253–255

Stern, M. S., Martin, P. D., Edwards, B. F. P., and Doscher, M. S. (1986) *Fed. Proc.* **45**, 1867

Tollin, P., Main, P., and Rossmann, M. G. (1966) *Acta Crystallogr. Sect. A. Cryst. Phys. Diffr. Theor. Gen. Crystallogr.* **20**, 404–407

Wlodawer, A. (1984) in *Biological Macromolecules and Assemblies* (Jurnak, F., and McPherson, A., eds) Vol. 2, pp. 393–439, John Wiley & Sons, New York

Wlodawer, A., and Sjölin, L. (1982) *Proc. Natl. Acad. Sci. U. S. A.* **79**, 1418–1422

Wlodawer, A., and Sjölin, L. (1983) *Biochemistry* **22**, 2720–2728

Wlodawer, A., Bott, R., and Sjölin, L. (1982) *J. Biol. Chem.* **257**, 1325–1332

Wlodawer, A., Miller, M., and Sjölin, L. (1983) *Proc. Natl. Acad. Sci. U. S. A.* **80**, 3628–3631

Wlodawer, A., Borkakoti, N., Moss, D. S., and Howlin, B. (1986) *Acta Crystallogr. Sect. B Crystollogr. Cryst. Chem.* **42**, 379–387

Wyckoff, H. W., and Richards, F. M. (1971) in *The Enzymes* (Boyer, P. D., ed) 3rd Ed., Vol. 4, pp. 647–806, Academic Press, New York

Wyckoff, H. W., Tsernoglou, D., Hanson, A. W., Knox, J. R., Lee, B., and Richards, F. M. (1970) *J. Biol. Chem.* **245**, 305–328